

Article

Comparison of Extrainsensitive Input Shaping and Swing-Angle-Estimation-Based Slew Control Approaches for a Tower Crane

Jan-Henri Montonen * , Niko Nevaranta , Markku Niemelä  and Tuomo Lindh 

School of Energy Systems, Lappeenranta-Lahti University of Technology (LUT), Skinnarilankatu 34, 53850 Lappeenranta, Finland; niko.nevaranta@lut.fi (N.N.); markku.niemela@lut.fi (M.N.); tuomo.lindh@lut.fi (T.L.)

* Correspondence: henri.montonen@lut.fi

Abstract: Tower cranes are needed to move heavy objects safely around construction sites. In tower cranes, payload oscillations are a typical problem that can cause safety issues, especially if the crane is not operated by an experienced user. Depending on the system, there are different causes for oscillations, e.g., inertial forces from the crane movement or external forces, such as weather conditions. Hence, the selected control law for input tracking plays an important role to limit the oscillatory motion and to help the crane operator to prevent unwanted operations. In this paper, we study the slew control of a tower crane application from the viewpoint of reducing payload oscillations. Two different approaches are studied: open-loop control based on extrainsensitive input shaping and closed-loop swing angle control, based on the estimation of the hoist cable angle. The proposed control approaches are validated by running the developed control program against a multibody mechanics simulator containing a model of a Liebherr tower crane. The studied control laws are also evaluated using an experimental setup, which consists of a two-axis manipulator, inverters, and a programmable logic controller in which the studied control methods are implemented. The results from the multibody dynamics simulations and from the experimental setup are presented and evaluated from the viewpoint of crane operation.

Keywords: input shaping; payload oscillations; swing angle estimation; slew control; tower crane



Citation: Montonen, J.-H.; Nevaranta, N.; Niemelä, M.; Lind, T. Comparison of Extrainsensitive Input Shaping and Swing-Angle-Estimation-Based Slew Control Approaches for a Tower Crane. *Appl. Sci.* **2022**, *12*, 5945. <https://doi.org/10.3390/app12125945>

Academic Editor: José Sánchez Moreno

Received: 3 May 2022

Accepted: 8 June 2022

Published: 10 June 2022

Publisher's Note: MDPI stays neutral with regard to jurisdictional claims in published maps and institutional affiliations.



Copyright: © 2022 by the authors. Licensee MDPI, Basel, Switzerland. This article is an open access article distributed under the terms and conditions of the Creative Commons Attribution (CC BY) license (<https://creativecommons.org/licenses/by/4.0/>).

1. Introduction

Tower cranes are widely used for lifting operations in different construction and industrial sites. During the operation of these cranes, the possible oscillatory behavior caused by the moving payload may have an adverse effect both on the accuracy of payload positioning and on safety. The control of these oscillations is a challenging task because of the nonlinear nature of the rotating system dynamics, and on the other hand, in most cases, there are not enough sensors to be used for compensation. This problem has been a topic of intense research in recent years and has resulted in several papers focusing on the modeling and control of various gantry and tower crane applications.

In the literature, various control approaches have been proposed to reduce the payload oscillations of different tower crane applications. The approaches can be roughly categorized into open- and closed-loop ones. The most straightforward methods are based on filtering of the natural frequencies from the trolley motion by using notch or low-pass filters [1]. The well-known input shaping can also be included in the same category as a method to modify the signal commands in order to minimize vibration [2]. Input shaping can be carried out in various ways, e.g., by creating multi-input-shaped commands [3], radial-motion-assisted shapers [4], or a zero-vibration shaper [5], to name but a few. The methods based on input shaping can be regarded as open-loop control methods, because the motion references are manipulated prior to being fed to controllers, and their main

advantage is that they do not require any measurement sensor for the payload angles. Different kinds of methods have also been proposed for input reference shaping, as in [6], where the authors use a model predictive controller to calculate optimal references for the inner loop PID control. The other category of approaches to reduce payload oscillations is closed-loop ones that are based on advanced control topologies, estimations, or additional feedback measurements. In [7], a neural-network-based control law is applied to a tower crane. Another approach is proposed in [8], where an elastic jib model for a large tower crane is derived and a state feedback law is proposed. In [9], a real-time optimal velocity control that is capable of limiting oscillations is presented. An inverse dynamics-based approach is introduced in [10] and compared with the traditional input shaper method. An observer-based nonlinear feedback controller for four-degree-of-freedom offshore ship-mounted tower cranes is proposed in [11]. A ship-mounted tower crane suffers from disturbances caused by sea waves or currents, which makes the controller design for such a system extra challenging. In [12], an adaptive sliding mode control is proposed for the antiswing control of a tower crane because of its robustness against system uncertainties and external disturbances. Further, in [13], an adaptive fuzzy control is proposed for the control of overhead cranes. The robustness of the method is tested with nonlinear disturbances. Due to the nature of disturbances (changing payloads, wind forces, collisions) in crane applications, it can be hard to measure the effect of disturbances on the crane system without extensive instrumentation. Adding extra instrumentation, on the other hand, is undesirable in the harsh environment in which the cranes operate. The control system must be designed robust enough to withstand these disturbances. Simulation of the effect of wind forces to a load carried by a mobile crane is presented in [14]. Although safety is not the primary aspect of this work, safety plays an important role in crane operations. Control system safety aspects of heavy industrial cranes are addressed and discussed in [15].

A crane should be able to transfer its payload quickly to the target position while suppressing the payload sway. The problem of load transfer is addressed in [16], where a control approach is proposed that is robust to variable rope length. Another approach, called saturating control, presented in [17], is used for suppressing the payload sway. In [18], a feedback control, based on inverse dynamics, is proposed to make the load follow a reference trajectory. Similar approach is often used in the control of industrial robot applications. In [19] an approach based on controlling the load position of an overhead crane instead of the trolley position, is presented for avoiding collisions of load with obstacles and to reduce load transfer time and residual vibration.

An antiswing control for crane application, based on swing angle feedback, is presented in [20]. Equations of motion for the load swing of a tower crane are presented in [21]. In this paper, the swing angle feedback control of [20] is combined with a swing angle estimator built from the equations presented in [21] to generate estimator-based swing angle feedback control. In this paper, we compare traditional input shaping and the estimator-based swing angle feedback control for reduction of payload oscillations of a tower crane. The comparison is conducted by using a virtual simulation tool and a small-scale experimental setup. Simulations are carried out using a multibody dynamics simulator environment with a model of a Liebherr 112EC-B8 tower crane. Both control approaches are also tested using a small-scale experimental laboratory setup, which has a belt-driven axis and a pendulum with angle measurement. This setup emulates one axis (trolley) of the tower crane movement. Although tower crane is used when comparing these methods, these methods can be adopted to other types of cranes, for example, gantry cranes and overhead cranes.

2. Slew Control Approaches

The tower crane has three degrees of freedom associated with the movement of the payload. The rotational motion of the movable jib is referred to as slew, the horizontal motion along with the jib as trolley, and the vertical movement of the payload as hoist as depicted in Figure 1a. The swing angle is the angle between the hoist cable and a

straight vertical line down from the trolley. The swing angle can be divided into radial and tangential components. Naturally, when the crane is operated, the movement of the payload may cause oscillatory behavior. Because this behavior is nonlinear in nature, the control of the unwanted oscillations is a difficult problem to solve. In most cases, there is not enough information, i.e., measurements from the system, in order to obtain a feedback-based control law. Thus, the derived control laws must be designed so that they reduce oscillations, e.g., by input reference shaping or by using estimator-based control strategies. In this paper, the slew motion of a tower crane application (see Figure 1a is analyzed from the viewpoint of reducing payload vibration by considering two different control approaches: (i) an open-loop robust extrainsensitive (EI) shaper and (ii) a slew-angle-estimation-based closed-loop method.

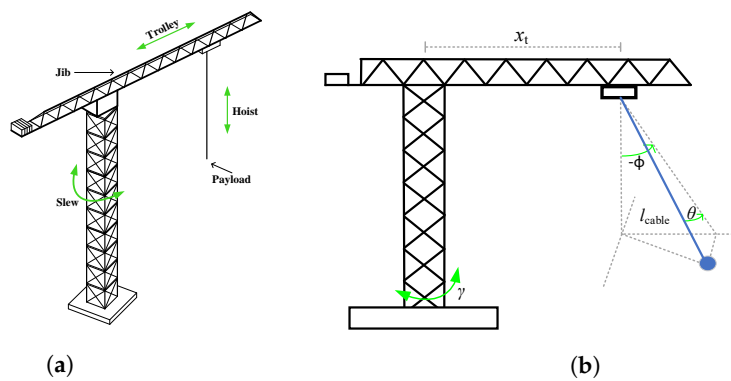


Figure 1. (a) Tower crane with three degrees of freedom: rotational movement (slew), horizontal movement (trolley), and vertical movement (hoist). (b) Simplified free body diagram of the dynamics.

2.1. Extrainsensitive Input Shaper

Input shaping is an open-loop approach for the slew control, and it consists of convolving of the input signal with well-chosen impulses. The basic idea is to compensate the oscillatory motion by shifted pulses

$$F(s) = A_0 + \sum_{i=1}^n A_i e^{-sT_i}, \tag{1}$$

where $A_0 \dots A_n$ and $T_1 \dots T_n$ are the amplitudes and time delays of the pulses. The basic principle of the input shaping approach is depicted in Figure 2b, where the velocity inner loop control $C(s)$ is a PID-based control. A block diagram of an input shaper is presented in Figure 2a. The input shaper consists of gains and delays. Different shapers can be obtained by changing the number of impulses and their amplitudes and delays. It is worth remarking that this method causes a lag to the operator's commands and makes operating of the crane somewhat more difficult.

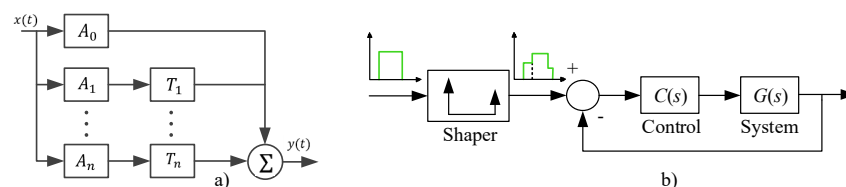


Figure 2. (a) Input shaper design using gains and delays and (b) input shaper used with the control.

In a tower crane system, the input shaping approach can reduce oscillations caused by inertial forces by modifying the reference signal. As real applications are often complicated to model accurately, the selected shaping approach should be designed so that it is robust to modeling errors and uncertainties. Different shaper designs have been presented in [22];

in the present paper, the extrainsensitive shaper (EI shaper) has been selected because of its insensitivity to modeling errors. Impulse amplitudes A and their delays t can be calculated as follows

$$EI = \begin{bmatrix} A_i \\ t_i \end{bmatrix} = \begin{bmatrix} \frac{1+V_{tol}}{4} & \frac{1-V_{tol}}{2} & \frac{1+V_{tol}}{4} \\ 0 & \frac{\tau}{2} & \tau \end{bmatrix}, \quad (2)$$

where V_{tol} is the maximum allowed residual vibration (e.g., 5% $\rightarrow V_{tol} = 0.05$), and τ is the period of undamped vibration. Residual vibration is the ratio of the vibration amplitude with input shaping to that without input shaping [22]. The period of undamped vibration can be calculated using

$$\tau = 2\pi\sqrt{\frac{l_{cable}}{g}} \quad (3)$$

where l_{cable} is the length of the hoist cable, and g is the gravitational acceleration. It is worth noticing that when the length of the hoist cable changes, its oscillation period changes. Therefore, delays of the shaper impulses must be changed accordingly. Depending on the shape of the load, the effective length of the hoist cable varies, and thereby the estimated or measured hoist cable length may differ. Thus, the robustness is provided by the selected EI-based input shaper structure.

2.2. Swing-Angle-Estimation-Based Closed-Loop Control

A swing angle feedback control is also studied in this paper. The method is based on the estimation of the hoist cable swing angle that is fed back to modify the speed reference to the speed controller. The slew and the trolley axis have their own independent speed control loops with a swing angle estimator. The estimator uses the radial and tangential acceleration of the trolley to calculate the estimated swing angle. Equations for the tangential and radial swing angles are derived in [21], and they are linearized for small swing angles by replacing $\sin(\theta)$ with θ . The estimated radial swing angle $\hat{\phi}$ (caused by the trolley movement, see Figure 1b) can be calculated from

$$\hat{\phi} = \frac{a_t - g\phi}{l_{cable}}, \quad (4)$$

where a_t denotes acceleration of the trolley, g is the gravitational force constant, and l_{cable} is the length of the hoist cable. The estimated tangential swing angle $\hat{\theta}$ (caused by the slew motion, see Figure 1b) can be calculated from

$$\hat{\theta} = \frac{x_t\omega_b - g\theta}{l_{cable}}, \quad (5)$$

where x_t denotes the trolley position (distance from the pivot point), ω_b is the rotational acceleration of the boom, and θ is the tangential swing angle of the hoist cable. It should be noted from (5) that the position of the trolley is required for the estimation of the tangential swing angle. The closed-loop approach is depicted in Figure 3, where the estimated value is used as a feedback for the PID velocity control. The PID controller controls the velocity of the associated axis according to the reference. The controller itself is a standard parallel-form PID controller. In the studied approach, the closed-loop controllers for the slew and the trolley movement use the estimated values as feedbacks, and they are working independent from each other. The estimated value is scaled by a gain K to obtain a suitable control effort. The gain can be different for each axis (K_ϕ for the radial and K_θ for the tangential axis). A rough guide for selecting an initial value for the parameter K is that it should produce approx. 50% of the maximum speed reference of the speed control when the swing angle is at its expected maximum. For example, if the maximum expected swing angle is 5 degrees, and the speed reference to the motor is between $-1...1$, a good initial

value for the tuning parameter K would be 0.1 ($0.1 \times 5 = 0.5$). The control error for the trolley movement e_t can then be expressed as

$$e_t = \omega_{ref,t} - \omega_t - K_\phi \cdot \hat{\phi}, \quad (6)$$

where $\omega_{ref,t}$ is the speed reference to the trolley motor, ω_t is the actual speed of the trolley motor, $\hat{\phi}$ is the estimated radial component of the swing angle, and K_ϕ is the tuning parameter on how much the swing angle affects the speed control error of the trolley motor. The equation is similar in the case of slew motion (tangential), but the variables are only replaced by the variables for slew motion.

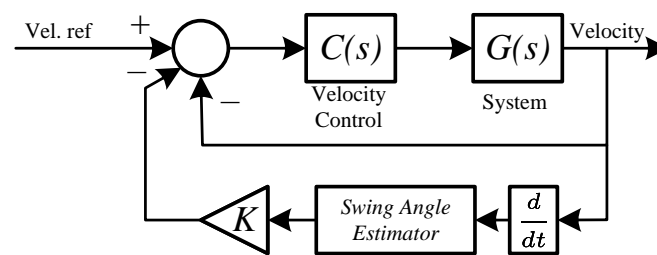


Figure 3. Proposed closed-loop method with a swing angle estimator. Acceleration of the trolley is the input to the estimator. It outputs the estimated angle, which is then multiplied by a tuning parameter K .

The hoist cable length is required for the estimation of the swing angles. However, it can be estimated by using information on the velocity of the hoist motor and mechanics of the hoist system. The initial position can be identified by performing an identification run at the system power-up, e.g., by raising or lowering the hook to its highest or lowest position and resetting the position to that.

3. Simulation Results

The tower crane control algorithms are simulated using a multibody dynamics simulator built by Mevea Ltd. (shown in Figure 4a). A Liebherr 112EC-B8 tower crane and a training area are modeled in the simulator, as the model and the simulator are also used for operator training (see Figure 4b). The multibody dynamics simulator communicates via an Ethernet connection with a relaying program. This relaying program connects to the Crane Control software, which is used for the implementation of the control algorithms and the user interface for changing control parameters. From the relaying program, it is possible to route signals to a programmable logic controller (PLC) and connect the actual hardware to the simulation loop. For example, one of the virtual motor drives of the crane can be substituted with a real one, i.e., modified to a hardware-in-loop (HIL) simulation [23]. However, the tests carried out in this paper are conducted without HIL simulation, and thus only the software components are used to model the crane. The simulation environment used in this study is presented in detail in [24].

The studied slew control approaches, namely the EI-shaper-based open-loop control and the swing-angle-estimator-based closed-loop control, are simulated and evaluated by considering similar operating conditions. The length of the cable is set to a constant value $l_{cable} = 19.2$ m to represent low-frequency oscillations, and the trolley position is kept constant. A barrel (mass 100 kg) is used as a load. The performance of the approaches is evaluated by means of residual vibrations at the end position of the motion profile.



Figure 4. (a) Cabin of the multibody dynamics simulator and (b) model of a Liebherr 112EC-B8 tower crane.

3.1. Shaper-Based Control

In Figure 5, the results of the input shaper are shown when the delays and amplitudes of the three impulses of the shaper have been tuned using the selected cable length and a residual vibration tolerance value of 5%, $V_{tol} = 0.05$. Figure 5a illustrates the situation without the shaper when the crane operator rotates the boom at the maximum velocity for about 15 s. Obviously, the load oscillatory movement is observable as the load swings heavily during the movement, and after the motion profile, a residual oscillation with an amplitude of 3.7 degrees is seen. In contrast, in Figure 5b, the EI shaper is applied, which significantly reduces oscillations in the system, as can be seen in the reduced residual vibrations. With the input shaper, the residual vibration is reduced to approximately 11% of the residual vibration without shaping.

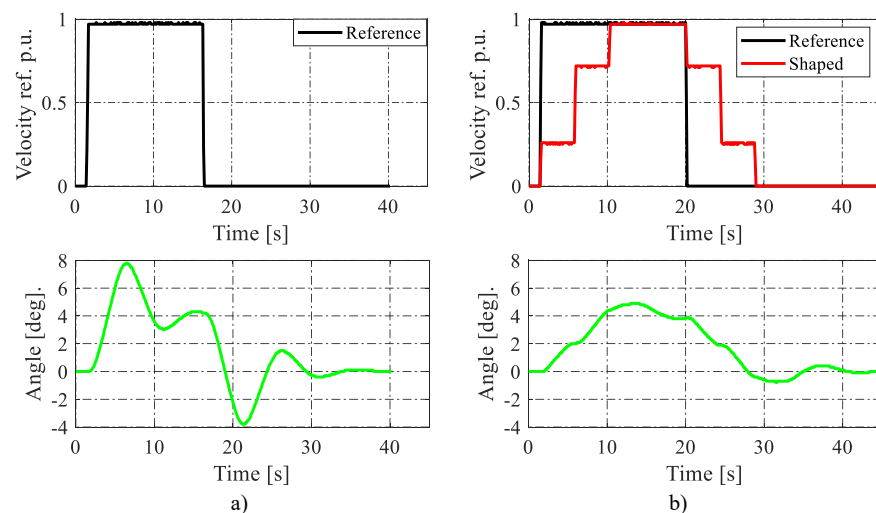


Figure 5. (a) Full slew movement without the input shaper and (b) results obtained with the EI input shaper method.

To further analyze the robustness properties of the EI-shaper-based approach, the actual cable length l_{cable} is varied and the shaper is designed using different design values l_{design} . The hoist cable length is considered the main source of uncertainty because its length varies greatly. Furthermore, the shape and size of the payload change the effective length of the hoist cable. In Figure 6, the results of four different tests are shown, where (a) the cable length is $l_{cable} = 5$ m and the shaper is designed using cable length value $l_{design} = 10$ m; (b) $l_{cable} = 5$ and $l_{design} = 15$ m; (c) $l_{cable} = 15$ and $l_{design} = 10$ m; and (d) $l_{cable} = 15$ m and $l_{design} = 20$ m. Based on the results with various operating and design conditions, the residual vibration is low compared with the design without the shaper in Figure 5a. Thus, it is shown that the EI shaper provides good robustness properties.

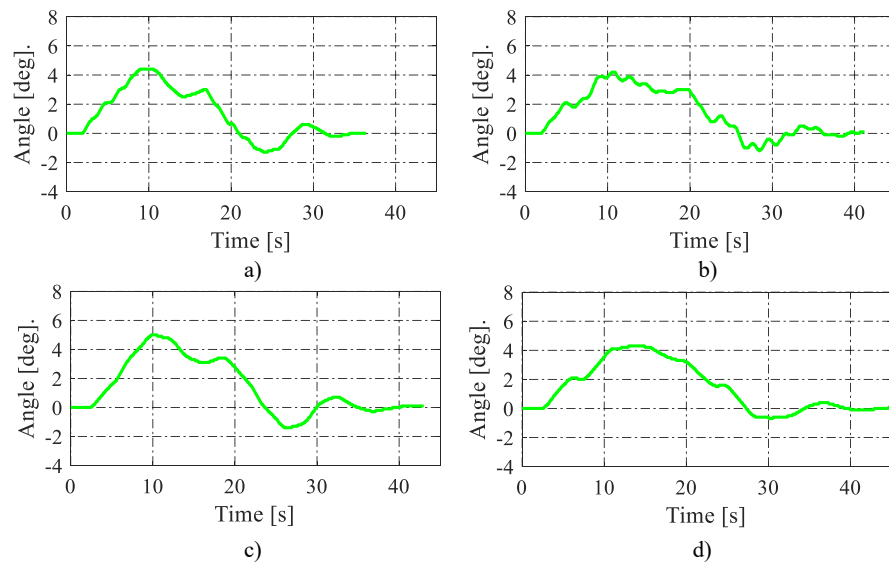


Figure 6. Analysis of the shaper design robustness against different actual cable lengths (l_{cable}): (a) $l_{cable} = 5$ m and $l_{design} = 10$ m; (b) $l_{cable} = 5$ m and $l_{design} = 15$ m; (c) $l_{cable} = 15$ m and $l_{design} = 10$ m; and (d) $l_{cable} = 15$ m and $l_{design} = 20$ m.

3.2. Swing-Angle-Estimation-Based Closed-Loop Control

The proposed closed-loop control based on the swing angle estimation is studied using the multibody dynamics simulator. In Figure 7, the results are shown (a) when the crane is operated only with the velocity control loop and (b) when the swing angle control is added to the system. A full-speed slew movement is used as a reference signal. The estimated swing angle is used as a feedback signal in the multibody dynamics simulator tests. The swing angle gain value (the tuning parameter K in Figure 3) is 5 for both the slew and the trolley movement ($K_\phi = K_\theta = 5$). The swing angle from measurement and estimation is in radians (degrees are used in figures), and the speed references to the slew and the trolley axis are in p.u. $-1...1$. The speed of the slew and the trolley motor is controlled by a PI controller. Swing angle estimation uses the actual hoist cable length.

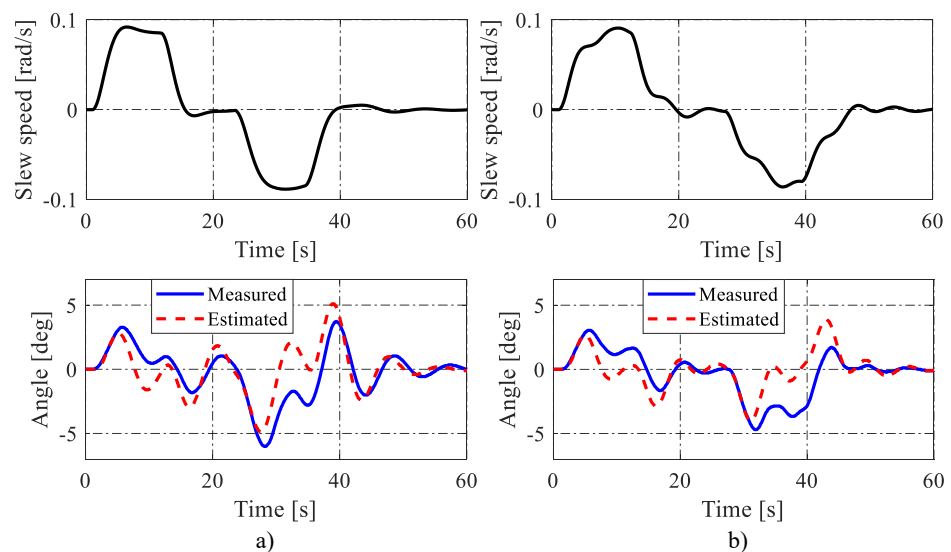


Figure 7. Comparison of control performance (a) without swing angle control and (b) with swing angle control.

According to Figure 7, the swing angle is overestimated compared with the measured swing angle. However, the control is capable of reducing the load swing without exact

swing angle information. The difference in amplitudes between the measured and the estimated swing angle can be compensated by using the swing angle gain value of the control. As long as the estimated swing angle has a correct sign during the acceleration and deceleration phases of the axis movement, the control is capable of reducing the load swing during these phases by slowing down or speeding up the axis and allowing the load to “catch up”. In Figure 7a, the different signs of the measured and the estimated swing angles at time $t = 10$ s and at $t = 32$ s are explained by air friction. As the cable and the load are moving through the air, it causes a small angle to the hoist cable in the simulator. The estimator does not take this into account, and it assumes that the load is swinging forward (in the direction of motion) when the acceleration ends and a constant speed is reached. Despite this, the residual vibration at the end of the motion is significantly reduced when using the feedback control.

4. Experimental Results

A two-axis manipulator setup is used as an experimental setup for verification of the tower crane control algorithms. The experimental system is depicted in Figure 8. The manipulator setup consists of two belt-driven axes, two ABB ACSM1 frequency converters, and an ABB AC500 PLC connected to the frequency converters via an EtherCAT fieldbus. A stiff rod is acting as the load of the crane. The rod is connected to a rotary encoder for swing angle measurement. It is worth remarking that there is only one axis of the manipulator in the experimental evaluation, because the rotary encoder allows to measure axis movement only in one direction. Therefore, the manipulator setup used here only emulates the trolley movement of the tower crane.

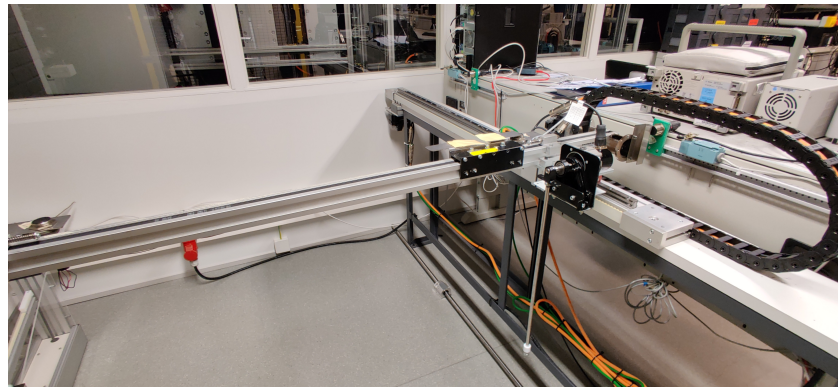


Figure 8. Experimental test setup emulating the trolley movement of the tower crane.

Both control methods are tested by implementing control algorithms to the PLC using the IEC61131-3 Structured Text language. A separate function generates a step up–step down speed reference to the axis in order to obtain comparable results. The function sets the speed reference to 10% of the nominal speed of the motor, which translates into approx. 0.79 m/s for 2 s and then zeros it. For data acquisition, the PLC sends reference values, actual values, and measured and estimated swing angles to a data logging computer. Figure 9 illustrates a test result when no control functions to suppress the oscillations are applied. Figure 9 also shows the estimated swing angle calculated using (4) by feeding the trolley movement to the equation.

As can be seen from Figure 9, the system oscillates heavily without supporting control functions. Next, an EI shaper is tuned to the system based on (2) and (3). With the maximum allowed residual vibration $V_{tol} = 0.05$ and by testing, we get an oscillation period $\tau = 1.56$ s for the pendulum. The vibration period is determined experimentally because the mass of the rod affects the center of gravity of the rod and weight system, and the equation for the vibration period of a mathematical pendulum as a function of pendulum length cannot be employed by using the total length of the rod and the load as the pendulum length. We

get impulse amplitudes $A_i = [0.2625 \ 0.475 \ 0.2625]$ and delays $T_i = [0 \ 0.78 \ 1.56]$ s for the EI shaper. The experimental test result using the EI shaper is presented in Figure 10.

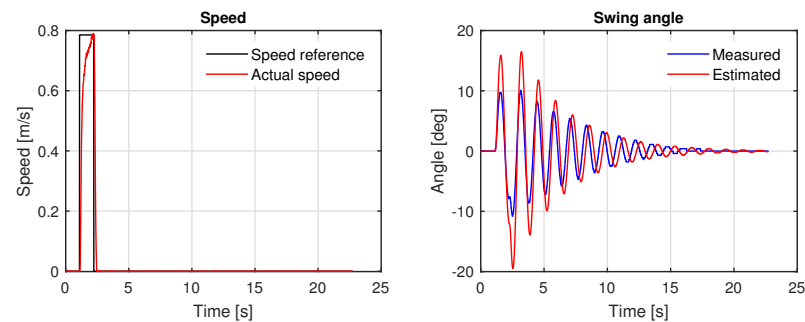


Figure 9. Speed reference and the actual speed (left) and the measured and estimated swing angles (right) when no control is applied.

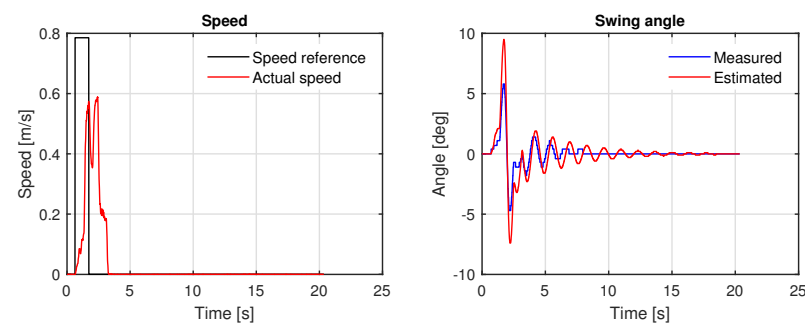


Figure 10. Speed reference and the actual speed and the measured and estimated swing angles when the EI shaper is applied.

As the results indicate, using a shaper to modify the input to the system significantly reduces load oscillations. The residual vibration (oscillation amplitude after the movement has ended) is approximately 10 degrees in the uncontrolled case, whereas the residual vibration is approximately 2 degrees when using an input shaper. The adverse effect of input shaping is visible in the shaped input signal as the trolley continues to move approximately 2 s after the reference signal has reached zero.

Next, the feedback-based control law is evaluated both by using direct measurement and estimation of the angle. Figure 11 presents a test result using the swing angle control law when the measured angle from the rotary encoder is used as a feedback. A swing angle gain value of 150 is used for the test, and it is kept the same in all tests. Using the feedback control reduces the delay in the operator commands compared with the input shaper. In this case, when using the actual measured angle from the sensor, the residual vibration is approximately the same as when using the input shaper shown in Figure 10. Next, the test result with the swing-angle-estimation-based feedback control is illustrated in Figure 12.

As can be noticed from the previous figures, the estimator overestimates the swing angle, which causes the system to react more strongly to the swing angle. This causes a slower movement and some correction action after the reference has reached zero but also small residual vibration. The value of the angle gain K_{Φ} was 150 during these tests; it is a tuning parameter that can be used to tune how much the control modifies the speed reference signal. It could even be a parameter that can be adjusted by the operator, as long as it has limits to prevent instability. The value of 150 used in the tests was selected experimentally.

As the load of the crane changes, the effective hoist cable length changes depending on the shape of the load. This causes an error between the actual and the assumed hoist cable length, which then affects the estimated swing angle. In Figure 13, robustness of the swing angle feedback control is tested by keeping the actual length of the rod and the load

system constant, but the l_{design} used in the estimator is varied. Results of the figure show that varying the hoist cable length (l_{cable}) between 80% and 120% of the actual length causes a residual vibration amplitude of 1 degree at worst.

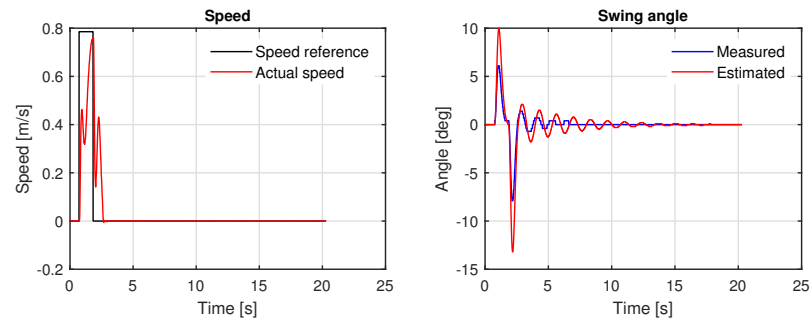


Figure 11. Speed reference and the actual speed and the measured and estimated swing angles when the swing angle feedback control using the measured angle is applied.

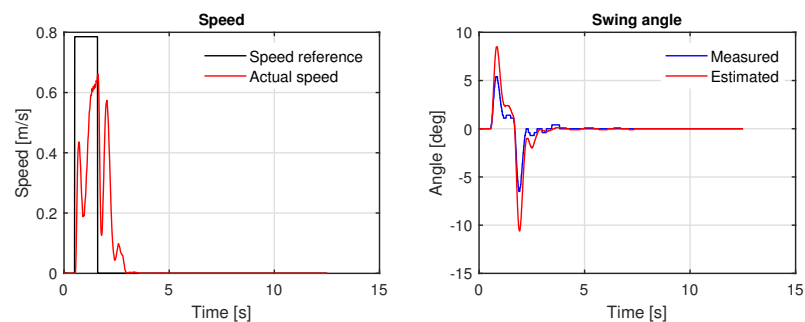


Figure 12. Speed reference and the actual speed and the measured and estimated swing angles when the swing angle feedback control using the estimated angle is applied.

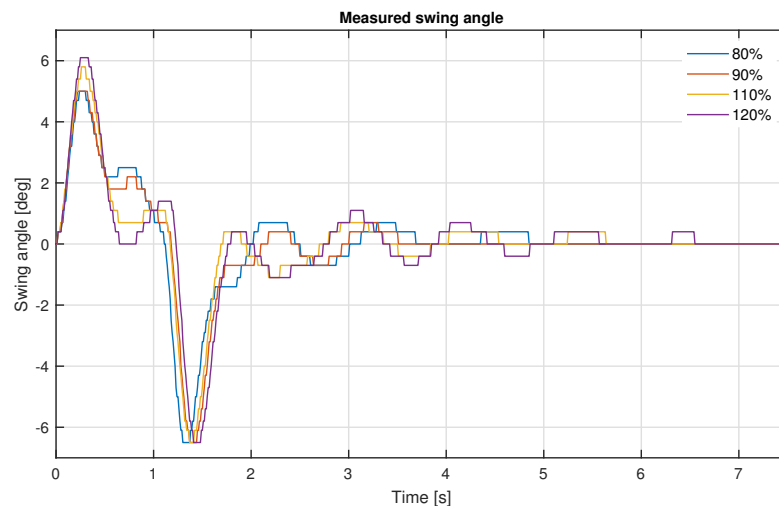


Figure 13. Measured swing angle when the hoist cable length is 80%, 90%, 110%, or 120% of the correct value.

5. Discussion

In this paper, we proposed methods for the swing angle control of a tower crane application with the main focus on reducing the payload oscillations. An extrainsensitive (EI) shaper and slew-angle-estimation-based closed-loop approaches were studied in a multibody simulator environment and by using an experimental small-scale setup.

The results indicate that although the input shaper suppresses load swing, it causes a long lag to the operator’s commands. Moreover, the lag is also dependent on the hoist cable

length. From the crane operator's viewpoint, this can be difficult to learn to compensate. For instance, when the values $l_{cable} = 19.2$ m and $V_{tol} = 0.05$ are used for the EI shaper design, the amplitudes are $A_0 = 0.2625$, $A_1 = 0.4750$, and $A_2 = 0.2625$ with delays $\tau_1 = 4.4$ s and $\tau_2 = 8.8$ s, respectively. When the full movement is operated with the joystick, only 26.25% of the control action takes place in real time, and when the second impulse starts to take effect, the crane moves on about 75% of the operators command.

As an alternative method, a swing-angle-feedback-based control was proposed. The simulation results show that the suggested method is as effective or better than the input shaper for reducing the load swing, without causing a noticeable lag to the operator commands. Although the estimated angle differs from the measured one, the swing angle feedback works well when using the estimated information, as long as the estimated angle has the same phase and roughly the same amplitude as the measured angle.

The hoist cable length naturally varies during lift operations; hence, the control algorithms must adapt to the changes. If not measured, the cable length can be estimated using the hoist motor speed and information on the mechanics of the hoist system if the initial position is known. The initial position can be recorded by performing an identification run every time the system is powered on, for example. Robustness of the estimated swing-angle-based feedback control for error in the hoist cable length was also shown. According to the results, varying the hoist cable length between 80% and 120% of the actual hoist cable length does not significantly affect the performance of the control. In tower cranes, using estimators reduces the need for sensors, as the need of sensors can be undesirable in harsh environmental conditions. Both of the compared methods suffer from external disturbances, such as the force of wind, as they have no information on external forces. Cranes typically have a wind anemometer installed, but the size and shape of payloads vary greatly, which makes it unreliable to estimate the force of wind acting on the payload.

Although a tower crane was used as a case example, this routine can also be adopted to other types of crane. For example, an overhead crane (also called bridge crane) has a similar construction to the experimental setup and has only trolley and hoist movement. In the future, it would be interesting to study the effect of changing the tuning parameter K to an adaptive value as in [25]. This would, however, mean that the performance of the control should be monitored, in other words, the swing angle should be measured. This might pose a problem in a real crane but not in an experimental setup.

Author Contributions: Conceptualization, J.-H.M., N.N. and T.L.; Methodology, J.-H.M., T.L. and N.N.; Software, J.-H.M.; Investigation, J.-H.M.; Writing—original draft preparation, J.-H.M. and N.N., Writing—review and editing, J.-H.M.; Supervision, T.L. and M.N., Funding acquisition, T.L. and M.N., Project administration, T.L. and M.N. All authors have read and agreed to the published version of the manuscript.

Funding: This research received no external funding.

Institutional Review Board Statement: Not applicable.

Informed Consent Statement: Not applicable.

Data Availability Statement: Not applicable.

Conflicts of Interest: The authors declare no conflict of interest.

References

1. Smith, A.D. Comparison of Filtering Methods for Crane Vibration Reduction. *Tower Undergrad. Res. J.* **2009**, *1*, 1–7.
2. Vaughan, J.; Kim, D.; Singhose, W. Control of Tower Cranes with Double-Pendulum Payload Dynamics. *IEEE Trans. Cont. Syst. Technol.* **2010**, *18*, 1345–1358. [[CrossRef](#)]
3. Vaughan, J.; Singhose, W. Reducing Vibration and Providing Robustness with Multi-Input Shapers. In Proceedings of the American Control Conference, Saint Louis, Mo, USA, 10–12 June 2009; pp. 184–189. [[CrossRef](#)]
4. Blackburn, D.; Lawrence, J.; Danielson, J.; Singhose, W.; Kamoi, T.; Taura, A. Radial-Motion Assisted Command Shapers for Nonlinear Tower Crane Rotational Slewing. *Control Eng. Pract.* **2010**, *18*, 523–531. [[CrossRef](#)]

5. Lawrence, J.; Singhose, W. Command Shaping Slewing Motions for Tower Cranes. *J. Vib. Acoust.* **2010**, *131*, 1–11. [[CrossRef](#)]
6. Bariša, T.; Bartulović, M.; Žužić, G.; Ileš, Š.; Matuško, J.; Kolonić, F. Nonlinear predictive control of a tower crane using reference shaping approach. In Proceedings of the 2014 International Power Electronics and Motion Control Conference and Exposition, Antalya, Turkey, 21–24 September 2014; pp. 872–876. [[CrossRef](#)]
7. Duong, S.C.; Uezato, E.; Kinjo, H.; Yamamoto, T. A Hybrid Evolutionary Algorithm for Recurrent neural network Control of a Three-Dimensional Tower Crane. *Autom. Constr.* **2012**, *23*, 55–63. [[CrossRef](#)]
8. Rauscheru, F.; Sawodny, O. An Elastic Jib Model for the Slewing Control of Tower Cranes. *IFAC-PapersOnLine* **2017**, *50*, 9796–9801. [[CrossRef](#)]
9. Devesse, W.; Ramteen, M.; Feng, L.; Wikander, J. A real-time optimal control method for swing-free tower crane motions. In Proceedings of the IEEE International Conference on Automation Science and Engineering (CASE), Madison, WI, USA, 17–20 August 2013; pp. 336–341. [[CrossRef](#)]
10. El-Badawy, A.A.; Shehata, M.M.G. Anti-sway control of a tower crane using inverse dynamics. In Proceedings of the 2014 International Conference on Engineering and Technology (ICET), Cairo, Egypt, 19–20 April 2014; pp. 1–6. [[CrossRef](#)]
11. Qian, Y.; Fang, Y. Switching Logic-Based Nonlinear Feedback Control of Offshore Ship-Mounted Tower Cranes: A Disturbance Observer-Based Approach. *IEEE Trans. Autom. Sci. Eng.* **2019**, *16*, 1125–1136. [[CrossRef](#)]
12. Bai, W.W.; Ren, H.P. Horizontal positioning and anti-swinging control tower crane using adaptive sliding mode control. In Proceedings of the 2018 Chinese Control And Decision Conference (CCDC), Shenyang, China, 9–11 June 2018; pp. 4013–4018. [[CrossRef](#)]
13. Chang, C.Y. Adaptive Fuzzy Controller of the Overhead Cranes with Nonlinear Disturbance. *IEEE Trans. Ind. Inform.* **2007**, *3*, 164–172. [[CrossRef](#)]
14. Cekus, D.; Gnatowska, R.; Kwiatkoń, P. Impact of Wind on the Movement of the Load Carried by Rotary Crane. *Appl. Sci.* **2019**, *9*, 3842. [[CrossRef](#)]
15. Slutej, A.; Kolonić, F.; Matuško, J.; Ileš, Š. Control of safety critical heavy industrial applications. In Proceedings of the 2014 16th International Power Electronics and Motion Control Conference and Exposition, Antalya, Turkey, 21–24 September 2014; pp. 958–962. [[CrossRef](#)]
16. Yoshida, K.; Matsumoto, I. Load transfer control for a crane with state constraints. In Proceedings of the 2009 American Control Conference, St. Louis, MO, USA, 10–12 June 2009; pp. 2551–2557. [[CrossRef](#)]
17. Teel, A. Using Saturation to Stabilize a Class of Single-Input Partially Linear Composite Systems. In Proceedings of the 2nd IFAC Symposium on Nonlinear Control Systems Design 1992, Bordeaux, France, 24–26 June 1992; pp. 379–384. [[CrossRef](#)]
18. Yanai, N.; Yamamoto, M.; Mohri, A. Feed-back control of crane based on inverse dynamics calculation. In Proceedings of the 2001 IEEE/RSJ International Conference on Intelligent Robots and Systems. Expanding the Societal Role of Robotics in the Next Millennium (Cat. No. 01CH37180), Maui, HI, USA, 29 October - 03 November 2001 ; Volume 1, pp. 482–487. [[CrossRef](#)]
19. Terashima, K.; Kaneshige, A. Load-position control of overhead travelling crane in terms of fixed-pole approach for 3-D transfer path. In Proceedings of the 1999 European Control Conference (ECC), Karlsruhe, Germany, 31 August–3 September 1999; pp. 1070–1075. [[CrossRef](#)]
20. Halder, B. Anti-Swing Control of a Suspended Varying Load with a Robotic Crane. Master's Thesis, Russ College of Engineering and Technology of Ohio University, Athens, OH, USA, 2002.
21. Omar, H.M. Control of Gantry and Tower Cranes. Ph.D. Thesis, Virginia Polytechnic Institute and State University, Blacksburg, VA, USA, 2003.
22. Vaughan, J.; Yano, A.; Singhose, W. Comparison of robust input shapers. *J. Sound Vib.* **2008**, *315*, 797–815. [[CrossRef](#)]
23. Lindh, T.; Montonen, J.H.; Niemelä, M.; Nokka, J.; Laurila, L.; Pyrhönen, J. Dynamic performance of mechanical-level hardware-in-the-loop simulation. In Proceedings of the 2014 16th European Conference on Power Electronics and Applications, Lappeenranta, Finland, 26–28 August 2014; pp. 1–10. [[CrossRef](#)]
24. Baharudin, E.; Nokka, J.; Montonen, H.; Immonen, P.; Rouvinen, A.; Laurila, L.; Lindh, T.; Sapanen, J.; Pyrhönen, J. Simulation Environment for the Real-Time Dynamic Analysis of Hybrid Mobile Machines. In Proceedings of the 11th International Conference on Multibody Systems, Nonlinear Dynamics, and Control, Boston, MA, USA, 2–5 August 2015; Volume 6, pp. 1–11.
25. Soriano, L.A.; Rubio, J.d.J.; Orozco, E.; Cordova, D.A.; Ochoa, G.; Balcazar, R.; Cruz, D.R.; Meda-Campaña, J.A.; Zacarias, A.; Gutierrez, G.J. Optimization of Sliding Mode Control to Save Energy in a SCARA Robot. *Mathematics* **2021**, *9*, 3160. [[CrossRef](#)]